Int. J. of GEOMATE, June, 2013, Vol. 4, No. 2 (Sl. No. 8), pp. 505-510
Geotec., Const. Mat. & Env., ISSN:2186-2982(P), 2186-2990(O), Japan

Application of PML to Analysis of Nonlinear Soil-Structure-Fluid Problem Using Mixed Element

Pahaiti Reheman[1], Hiroo Shiojiri[2],
[1]Graduated School of College of Science and Technology, Nihon University, Japan
[2]College of Science and Technology, Nihon University, Japan

ABSTRACT: Mixed element may be conveniently used to express non-linear constitutive equation of fluid and to avoid volumetric locking. X-FEM may be well suited to model discontinuity of displacements between solid and fluid. Appropriate boundary conditions should be set at the boundaries of numerical models not to reflect outgoing waves. In this paper, complex frequency shifted convolution-PML without splitting of variables is developed for mixed element, and the performances of PML are confirmed. The formulation of PML is completely consistent with corresponding FEM or X-FEM. It can be easily extended to any type of element and any nonlinear constitutive equations of the corresponding FEM or X-FEM. The resulting mass and stiffness matrices for PML are symmetric for linear models.

Keywords: Soil-structure-fluid interaction, X-FEM, Mixed formulation, Complex Frequency shifted PML

1. INTRODUCTION

Soil-structure-fluid interaction may have significant effects on seismic responses of structures. Mixed element may be conveniently used to express non-linear constitutive equation of fluid and to avoid volumetric locking. X-FEM may be well suited to model discontinuity of displacements between solid and fluid. In the X-FEM analysis, as well as FEM and FDM analyses, appropriate boundary conditions should be set at the boundaries of numerical models not to reflect outgoing waves.

Several methods are proposed (Wolf 1988). The first is the extensive mesh models using a finite element method or a finite difference method with approximate energy transmitting boundaries. The second is the substructure method using, for example, finite element and time domain boundary element method. In the former, the degrees of freedom of the models are often very large. The latter method may be more efficient, but the nonlinearity must be restricted within the nearby portion of structures modeled by finite element method, i.e. ,constitutive equations are assumed to be linear at and outer domain of the boundary. The third is FEM with PML or convoltion PML(Berenger 1994, Collino 2001,Basu 2003 2004,Drossaert 2007). PML and convolution PML are proved to have efficient wave absorbing capability for linear elasto-dynamic problem, and, the nonlinearity must be restricted within finite element domain. In the severe earthquakes, however, soil may become nonlinear to a large extent so that the second and the third methods may be inadequate. Convolutional PML is extended to cope with non-linear problem, so that nonlinear soil can be analyzed with a limited number of meshes without loss of accuracy (Shiojiri 2010, Reheman 2011). But, it is restricted to displacement based FEM.

Here, complex frequency shifted convolution-PML without splitting of variables is developed for mixed finite element and for X-FEM, and the performances of PML are confirmed. The formulation of PML is completely consistent with corresponding FEM or X-FEM. It can be easily extended to any type of element and any nonlinear constitutive equations of the corresponding FEM or X-FEM. The resulting mass and stiffness matrices for PML are symmetric for linear models.

2. METHOD

2.1 PML Formulation of Mixed Element for Fluid

Assuming that the effect of viscosity is negligible and that change of density is small, the equations of motion of fluid is given as:

$$\rho_0 \ddot{u}_i + \frac{\partial}{\partial x_i} p = 0 \tag{2.1}$$

,where ρ_0 is time averaged density of fluid, p is dynamic pressure, u_i is with component of displacement, and x_i denotes i th coordinate. Relationship between density and displacements is given as:

$$\rho + \rho_0 \sum_i \frac{\partial u_i}{\partial x_i} = 0 \tag{2.2}$$

,where ρ is difference between current density and time averaged decity. Relationship between dynamic pressure and ρ is expressed as follows.

$$p = f(\rho) \tag{2.3}$$

,where $f(\rho)$ is given as:

$$f(\rho) = c^2 \rho \quad \text{for} \quad p > p_v - p_0 \tag{2.3a}$$

$$f(\rho) = (\beta_0 c)^2 \rho + (1 - {\beta_0}^2)(p_v - p_0) \quad \text{for} \quad p < p_v - p_0 \tag{2.3b}$$

,in which c is velocity of sound, p_v is vapor pressure, p_0 is static pressure ,and β_0 is reduction ratio of sound velocity after cavitation.

Following the PML procedure, we introduce complex coordinate stretching function in frequency domain as:

$$\tilde{x}_i = \int_0^{x_i} \lambda_i(s)ds \qquad (2.4)$$

, where x_i denotes i th coordinate, and $\tilde{x}_i$ the corresponding transformed coordinate, and λ_i is given as:

$$\lambda_i = k_i + \frac{\sigma_i}{\alpha_i + i\omega} \qquad (2.5)$$

, where i is pure imaginary number, ω circular frequency, and k_i, α_i and σ_i non-negative continuous functions, such that k_i=1, and σ_i=0 at FEM-PML interface. At first, all equations are formulated in $\tilde{x}_i$ coordinate in frequency domain, and then transformed to x_i coordinate.

Equations of motion are given as:

$$-\omega^2 \rho_0 \bar{u}_i + \frac{\partial}{\partial \tilde{x}_i} \bar{p} = 0 \qquad (2.6)$$

,where ω is circular frequency, and $\bar{u}$ and $\bar{p}$ are displacement and pressure amplitudes in frequency domain respectively. The relationship between density and displacement are given as:

$$\bar{\rho} + \rho_0 \sum_i \frac{\partial \bar{u}_i}{\partial \tilde{x}_i} = 0 \qquad (2.7)$$

,where $\bar{\rho}$ is relative density amplitudes in frequency domain. Considering $\partial / \partial \tilde{x}_i = (1/\lambda_i)\partial / \partial x_i$, and multiplying both sides of Eqn.2.6 and Eqn.2.7 by $\lambda_1 \lambda_2$,we get;

$$-\lambda_1 \lambda_2 \omega^2 \rho_0 \bar{u}_i + \lambda_{\not{i}} \frac{\partial \bar{p}}{\partial x_i} = 0 \qquad (2.8)$$

$$\lambda_1 \lambda_2 \bar{\rho} + \rho_0 \sum_i \left(\lambda_{\not{i}} \frac{\partial \bar{u}_i}{\partial x_i} \right) = 0 \qquad (2.9)$$

,where $\not{i}$ denotes an integer other than i. Introducing weight functions w_i for displacements, and q for pressure, weak form equations for Eqn.2.8 and Eqn.2.9 are given as follows.

$$-\int_V w_i \lambda_1 \lambda_2 \omega^2 \rho_0 \bar{u}_i dv - \int_V \frac{\partial w_i}{\partial x_i} \lambda_{\not{i}} \bar{p} dv = -\int_S w_i n_i \lambda_{\not{i}} \bar{p} ds \qquad (2.10)$$

$$\int_V q\left(p - f(\rho)\right) dv = 0 \qquad (2.11)$$

Considering the fact that $-\omega^2$, $i\omega$,and $k_1 + \sigma_1/(\alpha_1 + i\omega)$ in frequency domain corresponds to d^2/dt^2, d/dt ,and $k + \sigma e^{-i\alpha t} *$ in time domain, equations in time domain are written as:

$$\begin{aligned} &\int_v \rho_0 w_i \left\{ k_1 k_2 \ddot{u}_i + \sum_j \frac{k_{\not{j}} \sigma_j (\alpha_{\not{j}} - \alpha_j) + \sigma_1 \sigma_2}{\alpha_{\not{j}} - \alpha_j} e^{-\alpha_j t} * \ddot{u}_i \right\} dv \\ &- \int_V \frac{\partial w_i}{\partial x_i} \left(k_{\not{i}} p + \sigma_{\not{i}} e^{-\alpha_{\not{i}} t} * p \right) dv \\ &= -\int_S w_i n_i \left(k_{\not{i}} p + \sigma_{\not{i}} e^{-\alpha_{\not{i}} t} * p \right) ds \end{aligned} \qquad (2.12)$$

$$\begin{aligned} &\kappa_1 \kappa_2 \rho + \sum_j \frac{k_{\not{j}} \sigma_j (\alpha_{\not{j}} - \alpha_j) + \sigma_1 \sigma_2}{\alpha_{\not{j}} - \alpha_j} e^{-\alpha_j t} * \rho \\ &= -\rho_0 \sum_i \left(k_{\not{i}} \frac{\partial u_i}{\partial x_i} + \sigma_{\not{i}} e^{-\alpha_{\not{i}} t} * \frac{\partial u_i}{\partial x_i} \right) \end{aligned} \qquad (2.13)$$

,where * denotes convolution integral. Denoting $e^{-\alpha t} * f(t) = \int_0^t e^{-\alpha(t-t')} f(t') dt' = F(t)$,

and introducing approximation

$F(t+\Delta t) = \Delta t \left\{ (1-\theta) e^{-\alpha \Delta t} f(t) + \theta f(t+\Delta t) \right\} + e^{-\alpha \Delta t} F(t)$,

we get

$$\begin{aligned} &\int_v \rho_0 w_i r_{12} \ddot{u}_i (t+\Delta t) dv \\ &+ \int_v \rho_0 w_i \sum_{j=1}^{2} U_{ij}^*(t) dv \\ &- \int_V \frac{\partial w_i}{\partial x_i} \left\{ r_{\not{i}} p(t+\Delta t) + P_{\not{i}}^*(t) \right\} dv \\ &= -\int_S w_i n_i \left\{ r_{\not{i}} p(t+\Delta t) + P_{\not{i}}^*(t) \right\} ds \end{aligned} \qquad (2.14)$$

,where

$r_{12} = k_1 k_2 + \theta \Delta t (k_2 \sigma_1 + k_1 \sigma_2)$, $r_{\not{i}} = k_{\not{i}} + \theta \Delta t \sigma_{\not{i}}$, and we define as followings:

$$\begin{aligned} P_{\not{i}}^*(t) &= \sigma_{\not{i}} \left\{ e^{-\alpha_{\not{i}} \Delta t} \int_0^t e^{-\alpha_{\not{i}}(t-t')} p(t') dt' + e^{-\alpha_{\not{i}} \Delta t} \Delta t (1-\theta) p(t) \right\} \\ &= e^{-\alpha_{\not{i}} \Delta t} \left\{ P_{\not{i}}^*(t-\Delta t) + \Delta t \sigma_{\not{i}} p(t) \right\} \end{aligned} \qquad (2.15)$$

$$\begin{aligned} U_{ij}^*(t) &= \frac{k_{\not{j}} \sigma_j (\alpha_{\not{j}} - \alpha_j) + \sigma_1 \sigma_2}{\alpha_{\not{j}} - \alpha_j} \left\{ e^{-\alpha_j \Delta t} \int_0^t e^{-\alpha_j (t-t')} \ddot{u}_i (t') dt' + e^{-\alpha_j \Delta t} \Delta t (1-\theta) \ddot{u}_i (t) \right\} \\ &= e^{-\alpha_j \Delta t} \left\{ U_{ij}^*(t-\Delta t) + \Delta t \frac{k_{\not{j}} \sigma_j (\alpha_{\not{j}} - \alpha_j) + \sigma_1 \sigma_2}{\alpha_{\not{j}} - \alpha_j} \ddot{u}_i (t) \right\} \end{aligned} \qquad (2.16)$$

Likewise, from Eqn.2.13,we get:

$$\begin{aligned} &r_{12} \rho(t+\Delta t) + R_{12}(t) \\ &= -\rho_0 \sum_i r_{\not{i}} \frac{\partial u_i}{\partial x_i} (t+\Delta t) - V_{12}(t) \end{aligned} \qquad (2.17)$$

,where $R_{12}(t) = \sum R_i^*(t)$, $V_{12}(t) = \sum_i V_i^*(t)$,and

$R_i^*(t) =$, $e^{-\alpha_i \Delta t} [R_i^*(t-\Delta t) + \Delta t \rho(t) [k_{\not{i}} \sigma_i (\alpha_{\not{i}} - \alpha_i) + \sigma_1 \sigma_2 \} / (\alpha_{\not{i}} - \alpha_i)]$,

$V_i^*(t) = e^{-\alpha_i \Delta t} \left(V_i^*(t-\Delta t) + \Delta t \rho_0 \sigma_{\not{i}} \partial u_i / \partial x_i \right)$

From Eqn.2.17, Eqn.2.3a,and Eqn.2.11,we get,

$$\int_V q\left\{r_{12}p(t+\Delta t)+\rho_0c^2\sum_j r_{\mp}\frac{\partial u_j}{\partial x_j}(t+\Delta t)\right\}dv=$$
$$-\int_V qc^2\left\{R_{12}(t)+V_{12}(t)\right\}dv$$

(2.18)

Discritizing domain of analysis by finite element, adopting Galerkin's formulation, and let $\mathbf{u}^e$, $\mathbf{P}^e$ $\mathbf{N_s}$ and $\mathbf{N_p}$ denote displacement and pressure vector at nodal points of a element, and interpolation matrices for displacement and pressure ,respectively, matrix form equations are obtained. From Eqn.2.14, we get,

$$\rho_0\int_v r_{12}\mathbf{N_s}^T\mathbf{N_s}dv\ddot{\mathbf{u}}^e(t+\Delta t)+\rho_0\int_v\mathbf{N_s}^T\mathbf{U}(t)dv$$
$$-\int_V\mathbf{B}^T\mathbf{R}_m\mathbf{N_p}dv\mathbf{P}^e(t+\Delta t)$$
$$-\int_V\mathbf{B}^T\mathbf{S}dv\mathbf{P}(t)$$
$$=-\int_S\mathbf{N_s}^T\mathbf{N}\mathbf{R}_m\mathbf{N_p}ds\mathbf{P}^e(t+\Delta t)$$
$$-\int_S\mathbf{N_s}^T\mathbf{N}\mathbf{S}ds\mathbf{P}(t)$$

(2.19)

,where

$$\mathbf{U}(t)=\begin{Bmatrix}\sum_{j=1}^{2}U_{1j}^*(t)\\ \sum_{j=1}^{2}U_{2j}^*(t)\end{Bmatrix},\mathbf{B}=\begin{bmatrix}\frac{\partial}{\partial x_1} & 0\\ 0 & \frac{\partial}{\partial x_2}\end{bmatrix}\mathbf{N_s},\mathbf{N}=\begin{bmatrix}n_1 & 0\\ 0 & n_2\end{bmatrix},$$

$$\mathbf{R}_m^T=\begin{bmatrix}r_2 & r_1\end{bmatrix},\mathbf{S}=\begin{bmatrix}\mathbf{N}_p & \mathbf{0}\\ \mathbf{0} & \mathbf{N}_p\end{bmatrix},\mathbf{P}(t)=\begin{Bmatrix}\mathbf{P}_2^*(t)\\ \mathbf{P}_1^*(t)\end{Bmatrix},$$

$$\mathbf{P}_i^*(t)=e^{-\alpha_i\Delta t}\left\{\mathbf{P}_i^*(t-\Delta t)+\Delta t\sigma_i\mathbf{P}^e(t)\right\}$$

From Eqn.2.18, we get,

$$\int_V r_{12}\mathbf{N_p}^T\mathbf{N_p}dv\mathbf{P}^e(t+\Delta t)$$
$$+\rho_0c^2\int_V\mathbf{N_p}^T\mathbf{R}_m^T\mathbf{B}dv\mathbf{u}^e(t+\Delta t)=\mathbf{R}(t)$$

(2.20)

,where

$$\mathbf{R}(t)=-c^2\left\{\int_V\mathbf{N_p}^T\mathbf{N_p}dv\mathbf{R}_{12}(t)+\int_V\mathbf{N_p}^TV_{12}(t)dv\right\}$$

、 $\mathbf{R}_{12}(t)=\mathbf{R}_1^*(t)+\mathbf{R}_2^*(t)$,and $\mathbf{R}_i^*(t)=$

$$e^{-\alpha_i\Delta t}[\mathbf{R}_i^*(t-\Delta t)+\Delta t\{k_{\mp}\sigma_i(\alpha_{\mp}-\alpha_i)+\sigma_1\sigma_2\}/\{(\alpha_{\mp}-\alpha_i)c^2\}\mathbf{P}^e(t)]$$

Let $\mathbf{H}$ and $\mathbf{G}$ be defined as

$\mathbf{H}=\int_V r_{12}\mathbf{N_p}^T\mathbf{N_p}dv,\ \mathbf{G}=\int_V\mathbf{N_p}^T\mathbf{R}_m^T\mathbf{B}dv$. Then,we get:

$$\rho_0\int_V r_{12}\mathbf{N_s}^T\mathbf{N_s}dv\ddot{\mathbf{u}}^e(t+\Delta t)$$
$$+\rho_0c^2\mathbf{G}^T\mathbf{H}^{-1}\mathbf{G}\mathbf{u}^e(t+\Delta t)$$
$$=-\int_S\mathbf{N_s}^T\mathbf{N}\mathbf{R}_m\mathbf{N}_pds\mathbf{P}^e(t+\Delta t)$$
$$-\int_S\mathbf{N_s}^T\mathbf{N}\mathbf{S}ds\mathbf{P}(t)$$
$$-\rho_0\int_V\mathbf{N_s}^T\mathbf{U}(t)dv+\mathbf{G}^T\mathbf{H}^{-1}\mathbf{R}(t)$$
$$+\int_V\mathbf{B}^T\mathbf{S}dv\mathbf{P}(t)$$

(2.21)

Element stiffness matrix $\rho_0c^2\mathbf{G}^T\mathbf{H}^{-1}\mathbf{G}$ has many hourglass mode and may lead to unstable solution. Since vorticity is preserved in non-viscous flow, and since fluid is assumed to be static in the beginning, the following equation is valid:

$$\varepsilon_c=\frac{\partial u_2}{\partial x_1}-\frac{\partial u_1}{\partial x_2}=0 \qquad (2.22)$$

So, in PML domain, the following equation is assumed.

$$\lambda_1\lambda_2\bar{\varepsilon}_c=\lambda_2\frac{\partial\bar{u}_2}{\partial x_1}-\lambda_1\frac{\partial\bar{u}_1}{\partial x_2} \qquad (2.23)$$

$$\lambda_2\frac{\partial\bar{\varepsilon}_c}{\partial x_1}=\lambda_1\frac{\partial\bar{\varepsilon}_c}{\partial x_2}=0 \qquad (2.24)$$

,where $\bar{\varepsilon}_c$ is amplitude of vorticity in frequency domain. Converting Eqn.2.23 into time domain ,and introducing approximation for convolution integral, we get,

$$r_{12}\varepsilon_c(t+\Delta t)+\sum_{j=1}^{2}\frac{k_{\mp}\sigma_j(\alpha_{\mp}-\alpha_j)+\sigma_1\sigma_2}{\alpha_{\mp}-\alpha_j}E_j^*(t)$$
$$=\sum_j\left\{(-1)^{j-1}r_{\mp}\frac{\partial u_{\mp}}{\partial x_j}(t+\Delta t)+U_{\mp j}^*(t)\right\}$$

(2.25)

,where

$\mathrm{E}_j^*(t)=e^{-\alpha_j\Delta t}\left\{\mathrm{E}_j^*(t-\Delta t)+\Delta t\varepsilon_c(t)\right\}$,

$U_{12}^*(t)=e^{-\alpha_1\Delta t}\left\{U_{12}^*(t-\Delta t)+\Delta t\sigma_1\partial u_1(t)/\partial x_2\right\}$, and

$U_{21}^*(t)=e^{-\alpha_2\Delta t}\left\{U_{21}^*(t-\Delta t)+\Delta t\Delta t\sigma_2\partial u_2(t)/\partial x_2\right\}$

. Introducing weight function w_1, w_2 and deriving weak form equation from Eqn.2.24,we get,

$$-\int_V\alpha\left(w_2\lambda_2\frac{\partial\bar{\varepsilon}_c}{\partial x_1}-w_1\lambda_1\frac{\partial\bar{\varepsilon}_c}{\partial x_2}\right)dv$$
$$=-\int_S\alpha\left(w_2n_1\lambda_2-w_1n_2\lambda_1\right)\bar{\varepsilon}_cds \qquad (2.26)$$
$$+\int_V\alpha\left(\lambda_2\frac{\partial w_2}{\partial x_1}-\lambda_1\frac{\partial w_1}{\partial x_2}\right)\bar{\varepsilon}_cdv=0$$

Transforming Eqn.2.26 into time domain equation, and introducing approximation for convolution integral, and substitutingEqn.2.25,we get,

$$\int_V\frac{\alpha}{r_{12}}\left(r_2\frac{\partial w_2}{\partial x_1}-r_1\frac{\partial w_1}{\partial x_2}\right)\left(r_2\frac{\partial u_2}{\partial x_1}(t+\Delta t)-r_1\frac{\partial u_1}{\partial x_2}(t+\Delta t)\right)dv$$
$$+\int_V\alpha\left(\frac{\partial w_2}{\partial x_1}\sigma_2E_2^*-\frac{\partial w_1}{\partial x_2}\sigma_1E_1^*\right)dv \qquad (2.27)$$
$$+\int_V\frac{\alpha}{r_{12}}\left(r_2\frac{\partial w_2}{\partial x_1}-r_1\frac{\partial w_1}{\partial x_2}\right)E(t)dv$$
$$=\int_S\alpha\left\{\left(w_2n_1r_2-w_1n_2r_1\right)\varepsilon_c+\left(w_2n_1\sigma_2E_2^*-w_1n_2\sigma_1E_1^*\right)\right\}ds$$

,where $E(t)=$

$$-\sum_{j=1}^{2}\{k_{\mp}\sigma_j(\alpha_{\mp}-\alpha_j)+\sigma_1\sigma_2\}E_j^*(t)/(\alpha_{\mp}-\alpha_j)+U_{21}^*(t)-U_{12}^*(t),$$

$\mathrm{E}_j^*(t)=e^{-\alpha_j\Delta t}\times$

$\left\{\mathrm{E}_j^*(t-\Delta t)+\Delta t\varepsilon_c(t)\right\},U_{12}^*(t)=e^{-\alpha_1\Delta t}\left\{U_{12}^*(t-\Delta t)+\Delta t\sigma_1\partial u_1(t)/\partial x_2\right\},$

and $U_{21}^*(t)=e^{-\alpha_2\Delta t}\times\left\{U_{21}^*(t-\Delta t)+\Delta t\Delta t\sigma_2\partial u_2(t)/\partial x_1\right\}$.

Introducing interpolation matrices, the following equations are obtained.

$$\int_V \frac{\alpha}{r_{12}} \mathbf{B_c}^T \mathbf{B_c} dv \mathbf{u}^e (t+\Delta t)$$

$$= -\int_V \alpha \mathbf{B_e}^T \begin{Bmatrix} E_1^* \\ E_2^* \end{Bmatrix} dv - \int_V \frac{\alpha}{r_{12}} \mathbf{B_c}^T E(t) dv$$

(2.28)

,where

$$\mathbf{B_c} = \begin{bmatrix} -r_1 \frac{\partial}{\partial x_2} & r_2 \frac{\partial}{\partial x_1} \end{bmatrix} \mathbf{N_s}, \mathbf{B_e} = \begin{bmatrix} -\sigma_1 \frac{\partial}{\partial x_2} & 0 \\ 0 & \sigma_2 \frac{\partial}{\partial x_1} \end{bmatrix} \mathbf{N_s}$$

By adding Eqn.2.21 and Eqn.2.28,we get final matrix form equations. Substituting interpolation function for X-FEM, we get PML for XFEM.

3 NUMERICAL EXAMPLE

3.1 Reservoir Model

Reservoir with 100m depth subjected to horizontal rigid wall motion is analyzed using proposed mixed formulation FE-PLM. Length of reservoir model varies from 100m to 600m. Boundary conditions assigned on upstream boundary are fixed boundary, viscous boundary with viscosity ρc, and PML. Meshes of models are shown in Fig.3.1~3.3. Meshes with sign x indicate PML. Forced horizontal vibration of rigid wall on the left end of reservoir is assumed. The results are shown in Fig.3.4~3.9. Fixed boundary results show strong dependency on the location of upstream boundary. The results with viscous boundary show less dependency on the location of boundary for 1Hz excitation, but large dependency for 5Hz excitation. Proposed PML boundary shows very little discrepancy between different boundary locations for both 1Hz and 5Hz excitation.

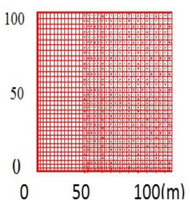
Fig.3.1 Reservor Mesh (length 100m)

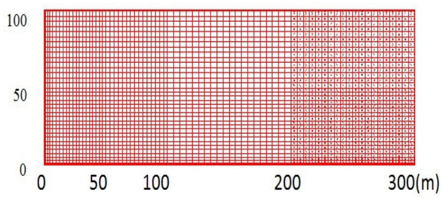
Fig.3.2 Reservor Mesh (length 300m)

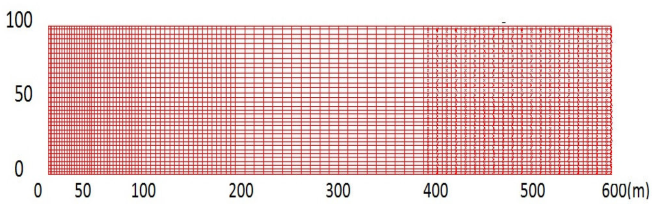
Fig.3.3 Reservor Mesh(length 600m)

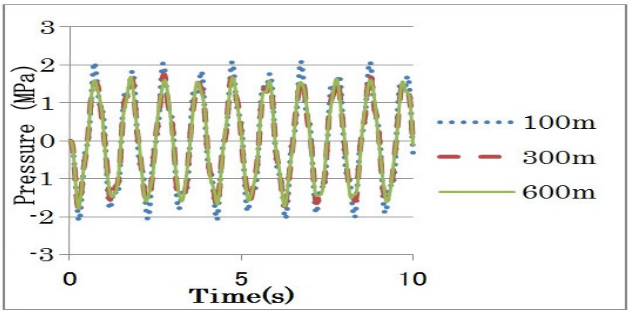

Fig.3.4 Fixed Boundary (1Hz)

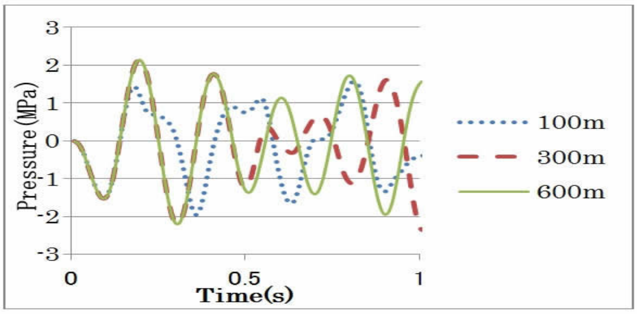

Fig.3.5 Fixed Boundary (5Hz)

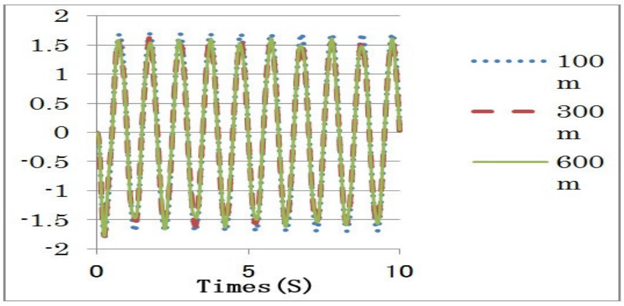

Fig3.6 Viscous boundary(5Hz)

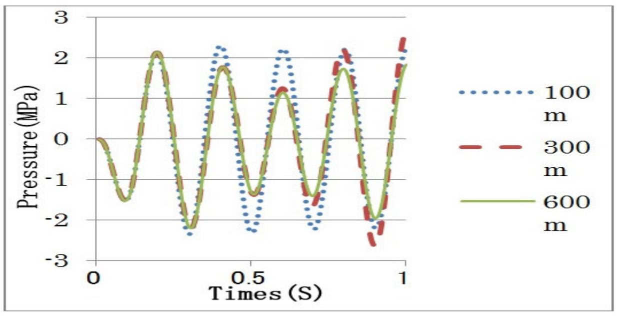

Fig3.7Viscous boundary(5Hz)

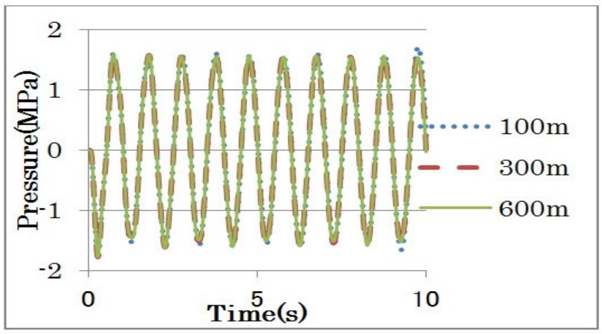

Fig 3.8 PML(1Hz)

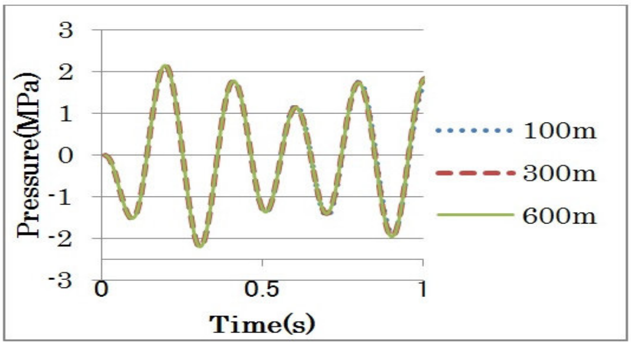

Fig3.9 PML(5Hz)

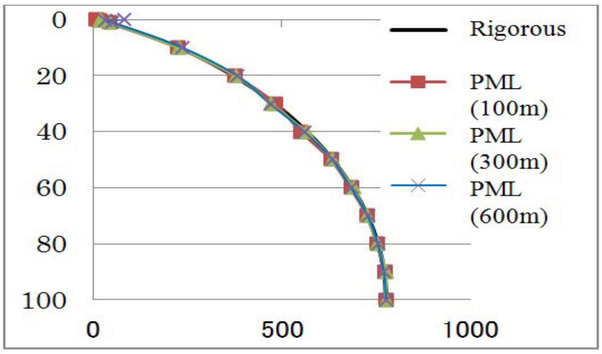

Fig 3.10 Pressure Distribution(1Hz)

3.2 Dam- Reservoir-Foundation Model

Dam-reservoir-foundation model was constructed using X-FEM for tangential discontinuity of displacement at solid-fluid interface ,and combining proposed mixed formulation FE-PML for fluid with FEM-PML for solid (Fig3.11) .Two kinds of mashes are used (Fig.3.12,Fig.3.13).

Discontinuous displacement in tangential direction near the top of dam is shown in Fig.14, indicating the effect of discontinuous interpolation function of X-FEM. In Fig.15-17, responses of dam top using two mesh models subjected to sinusoidal horizontal ground motion are compared. The results of two mesh model coincide each other, indicating that model size has little effect when proposed PML is used.

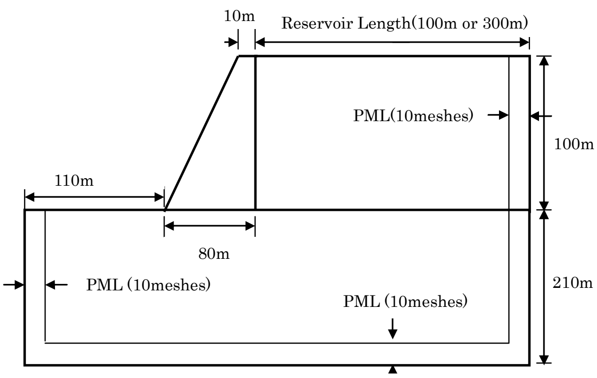

Fig 3.11 Dam-reservoir-foundation model

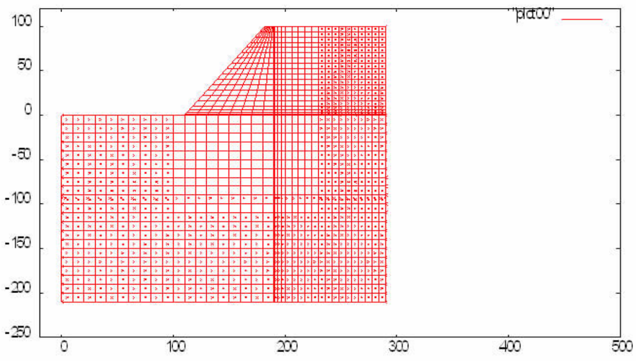

Fig 3.12 Meshes (reservoir length=100m)

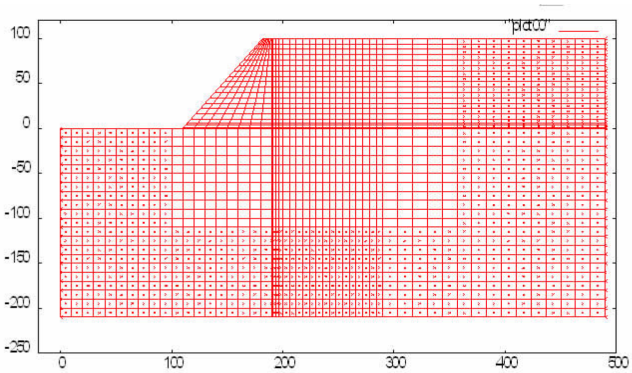

Fig 3.13 Meshes(reservoir length=300m)

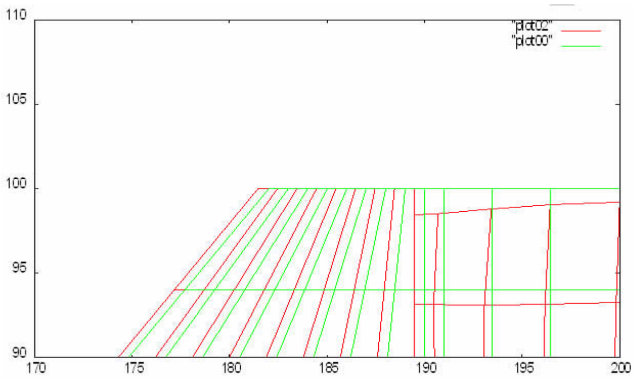

Fig 3.14 Displacements near top of dam

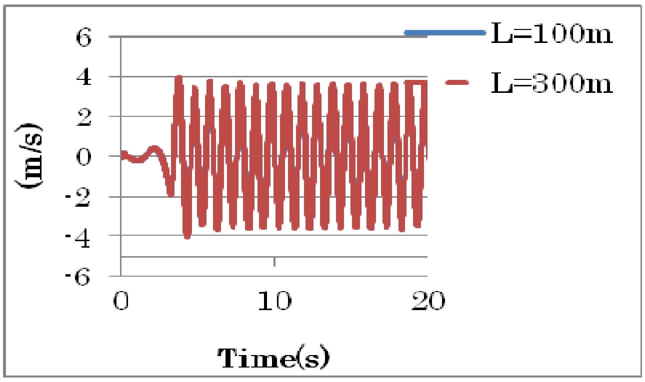

Fig 3.15 Response of dam top (1Hz)

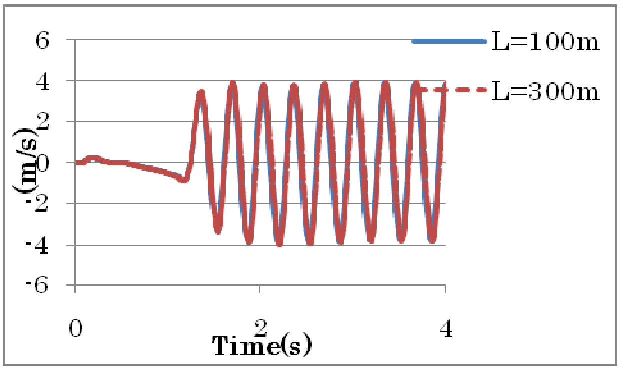

Fig 3.16 Response of dam top (3Hz)

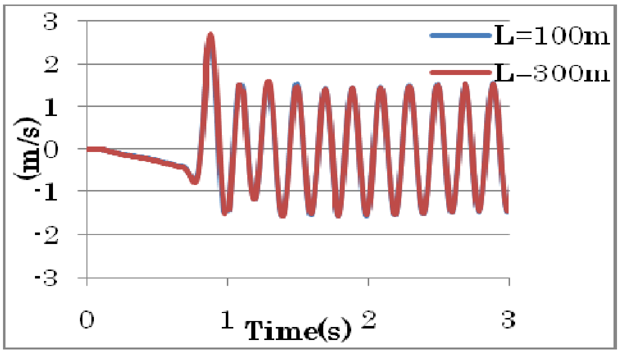

Fig 3.17 Response of dam top (5Hz)

4 CONCLUSION

Convolution PML based on mixed formulation is formulated and computer code is developed for FEM and X-FEM. It was applied to reservoir model and the performance of absorbing outgoing wave was much better than conventional boundary. By applying to dam-reservoir-foundation model including FEM and X-FEM, it was demonstrated that the formulation was quite general, and that it has wide class of application.

5 REFERENCES

[1] Wolf, J.P.(1988). Soil-Structure-Interaction Analysis in time Domain, Prentice-Hall, Engelwood Cliffs.

[2] Berenger P.(1994).A Perfectly Matched Layer for the Absorption of Electromagnetic Waves, Journal of Computational Physics, 114, 185-200..

[3] Collino,F. ,and Tsogka,C.(2001).Application of the perfectly matched absorbing layer to the linear elastodynamic problem in anisotropic heterogeneous media, Geophysics, 66 :1,294-307.

[4] Drossaert,F.H.,abd Giannopoulis,A.(2007) Complex frequency shifted convolution PMl for FTDT modeling of elastic waves, Wave Motion ,l.44:8593-604.

[5] Basu,U ,and Chopra, A.K.(2004),.Perfectly Matched layers transient elestodynamics of unbounded domains, Int.J.Numerical Methods Eng..59, 1039-1074.

[6] Basu,U. ,and Chopra, A.K.(2003), Perfectly matched layers for time-harmonic elesto dynamics of unbounded domains: theory and finite-element implementation, Comput. Methods Appl. Mech. Eng.192, 1337-1375.

[7] H.Shiojiri,,P.Reheman. & Li J.F.(2010) Application of PML for Non-Linear Soil-Structure Problem,. 14ECEE,Ohrid, 1-8CD.

[8] P. Reheman,H.SHIOJIRI, Jeng-Feng LI(2011) Analytical Method for Nonlinear Soil-Structure Interaction using PML,Eurodyne, Leuven, Belgium, 1-6CD.

Int. J. of GEOMATE, June, 2013, Vol. 4, No. 2 (Sl. No. 8), pp. 505-510.
MS No. 2167 received June 13, 2012, and reviewed under GEOMATE publication policies.

Pertinent discussion including authors' closure, if any, will be published in the June 2014 if the discussion is received by Dec., 2013.
Corresponding Author: Pahaiti Reheman